Article Title
Drive-by detection of railway track stiffness variation using in-service vehicles

Authors
Paraic Quirke
Daniel Cantero
Eugene J. OBrien
Cathal Bowe

Drive-by detection of railway track stiffness variation using in-service vehicles

Paraic Quirke[1,2], Daniel Cantero[3], Eugene J. OBrien[1], Cathal Bowe[2]

[1]School of Civil Engineering, University College Dublin, Dublin 4, Ireland.
[2]Iarnród Éireann Irish Rail, Technical Department, Engineering & New Works, Inchicore, Dublin 8, Ireland.
[3]Department of Structural Engineering, Norwegian University of Science & Technology, Trondheim, Norway.

email: paraic.quirke@irishrail.ie, daniel.cantero@ntnu.no, eugene.obrien@ucd.ie, cathal.bowe@irishrail.ie

ABSTRACT: Railway track stiffness is an important track property which can help with the identification of maintenance related problems. Railway track stiffness can currently be measured using stationary equipment or specialised low-speed vehicles. The concept of using trains in regular service to measure track stiffness, has the potential to provide inexpensive daily 'drive-by' track monitoring to complement data collected by less-frequent monitoring techniques.

A method is proposed in this paper for the detection of track stiffness variation through an analysis of vehicle accelerations resulting from the vehicle-track dynamic interaction (VTI). The Cross Entropy optimisation technique is applied to determine the track stiffness profile which generates a vehicle response that best fits the measured vertical accelerations of a railway carriage bogie.

Numerical validation of the concept is achieved by using a 2-dimensional half-bogie dynamic model, representing a railway vehicle, to infer a global track stiffness profile along a track. The Track Stiffness Measurement Algorithm (TSMA) is implemented in Matlab. This paper reports the results of the numerical simulations. The proposed method gives good estimates of the track stiffness. To the authors' knowledge this is the first time an optimisation technique has been applied to the determination of railway track stiffness.

KEY WORDS: Railway; Track; Stiffness; Drive-by; Vehicle Track Interaction; Cross Entropy.

1   INTRODUCTION

Using in-service trains to monitor the condition of railway infrastructure has been an emerging field of research since the early 2000s. Improvements in bandwidth of wireless communications, sensor robustness and electronics have allowed the development of unattended track geometry inspection systems that are compact and robust enough to be mounted on in-service vehicles.[1] A method is proposed in this paper to use sensors fixed to in-service trains to measure track stiffness. Track stiffness data, collected frequently, complements other track condition information and helps infrastructure managers to improve maintenance planning. Over time, analysis of data will identify track problems and can be used to determine rates of track condition deterioration allowing for timely intervention.

Railway track stiffness is an important track property which can help with the identification of problems related to track settlement, vehicle ride comfort, ground-borne vibrations and track geometry irregularities. Track stiffness can be defined in a number of ways. Considering the entire track structure, global track stiffness, k, can be defined as the ratio between track load, F, and track deflection, z at a point. However, it is accepted that track stiffness is non-linear as stiffness increases with increased loading.[2] Most track components have a non-linear behaviour, notably the behaviour of ballast under load. Voids under sleepers can also affect the global track stiffness value.

Railway track stiffness varies along a track. Dahlberg[3] summarises the factors influencing track stiffness variation. Global track stiffness is a term used when the entire track structure is considered, i.e. the combined stiffness of individual track components. Global track stiffness increases significantly at switches and crossings due to the use of wider sleepers giving greater load distribution and the changing rail bending stiffness due to the specific shape of the rail at these features. Transition zones between bridges and embankments exhibit rapid changes in global track stiffness. Differential track settlement occurring in the vicinity of switches and crossings, and railway bridge transition zones can be attributed to the sudden changes in track stiffness. A study into using under-sleeper pads of varying stiffnesses in transition zones between bridges and embankments is shown to reduce variations in wheel/rail contact forces generated by the rapid changes in track stiffness and reduce differential settlement.[4]

A railway track can be divided into two separate structures, the superstructure (rails, rail pads, sleepers) and the substructure (ballast, sub-ballast, subgrade, drainage systems).[5] The global track stiffness is influenced by the properties of the individual structural elements in the superstructure and substructure. The elements making up the superstructure have well defined and easily measurable properties and their individual contribution to the global track stiffness are well known. As the superstructure elements are visible from the surface, it easy to inspect them to identify defects which may contribute to variations in the global track stiffness value. The track substructure is less homogenous than the superstructure and unexpected variations in global track stiffness can often be attributed to variations in the properties of its constituent elements. As the elements of the substructure are concealed below the superstructure it is difficult to measure their properties in the field. Variations in ballast thickness, subgrade strength and the presence of groundwater due to poor drainage all contribute to variations in global track stiffness and are difficult to monitor. However, Selig and Li[6] show that the modulus of the subgrade is the dominant factor in determining the global track stiffness.

The performance of the substructure is heavily dependent on the subgrade performance, and regular track maintenance such as ballast cleaning or tamping does not correct a poor subgrade.[7] Track geometry defects associated with a poor subgrade tend to reappear relatively quickly meaning these regular track maintenance techniques can be costly and ineffective. Therefore it is important to have an understanding of the track stiffness in order to assess the subgrade performance so that more appropriate maintenance measures (mini-piles, subgrade replacement) can be chosen as appropriate.

Variation in track properties, including track stiffness, cause variations in the train/track dynamic interaction.[8] The train/track interaction is further magnified with increased vehicle loads and speeds. Fröhling[9] concludes from development of track deterioration prediction models that spatial variation of railway track stiffness contributes significantly to track deterioration, both in terms of differential track settlement and increased vehicle loading. Consequently, as track deterioration increases, the train/track dynamic interaction forces increase and the rate of track deterioration increases.

Historically, most standard measurement techniques involve the inspection of the superstructure. Until recently the substructure has been given less consideration, even though it has a major influence on the cost of track maintenance.[10] Current standard measurement techniques for condition monitoring of track require the measurement of track geometry using specialist recording cars. Track condition is determined through the evaluation of various parameters (gauge, longitudinal level, twist, etc.) and analysis to ensure these parameters are within certain threshold limits.[11] Large variations in track stiffness may exist on sections of track with high quality track geometry and these stiffness variations are not evident until the track is dynamically loaded by a train. Consequently, track geometry recording cars using optical measurement methods cannot be relied upon to identify all issues on a track and there is clearly a need to identify and measure variations in other track substructure properties such as track stiffness.

In recent years new measurement trains measuring the vehicle reaction to the track condition in addition to track geometry measurement have highlighted this issue. In Germany, Deutsche Bahn (DB) combine the two different measurement methods on board their InterCity Express –

Schnellfahrtzug (German for 'high speed train') ICE-S measurement train. An analysis of the correlation of defects detected by track geometry measurement and vehicle reaction measurement found that for 18% of the exceedances of vehicle reaction measurement limits, no abnormality could be found in the corresponding geometry measurement data.[12] This indicates that track substructure properties can be responsible for unacceptable vehicle vertical accelerations and yet cannot be detected by traditional measurement methods.

Current track stiffness measurement techniques can be divided into two categories: static measurement and dynamic measurement. Static measurement techniques such as falling weight deflectometer and dynamic cone penetration tests provide detailed stiffness information for the track subgrade at local areas of interest. However, creating a stiffness profile for longer sections of track using static techniques is time consuming, expensive, and generally requires a track possession. Murray *et al.* present a method of static track stiffness measurement using track side mounted cameras and digital image correlation to measure track deflection.[13] They report that foundation parameters can vary significantly over a short length of track. In test results presented the inferred track stiffness varies by a factor of 2 between adjacent sleepers. These variations could be attributed to a range of factors including poor ballast packing under the sleepers, voids creating hanging sleepers or sudden variations in ballast thickness between sleepers.

Efficiency in measurement can be greatly improved by adopting 'drive-by' or continuous measurement systems which provide:-

- Wide network coverage enabling the identification of problem areas for further detailed testing using static methods; and
- Stiffness measurements for loaded track providing a more realistic track response to the passage of regular trains.

Extensive research has been carried out into the development of specialised vehicles to measure track stiffness. As part of the INNOTRACK project a railway portancemetre was developed from a road portancemetre.[7] The portancemetre is a track-mounted towed apparatus featuring two vibrating wheels on the unsprung mass that generate dynamic loads similar to typical in-service vehicle axle loads. The magnitude and frequency of the load is adjusted to study the mechanical behaviour of the track. The applied force and displacement of the track are measured and the track stiffness calculated using the direct force-displacement curve method. Low operational speeds (3-10 km/h) mean that the use of this vehicle disrupts regular revenue making services.

The Rolling Stiffness Measurement Vehicle (RSMV), developed in Sweden, measures dynamic track stiffness up to 50 Hz. Two oscillating masses above the axle of a modified freight wagon excite the track dynamically. Vertical track stiffness is calculated from measured axle box accelerations and forces.[14] Overall stiffness measurements can be returned at measurement speeds of up to 60 km/h while detailed investigations can be undertaken at lower speeds (10 km/h). More recently, an additional system recording rail longitudinal levels at loaded and unloaded sections of track has been added to a standard measuring vehicle to enable track deflection/stiffness measurements.[15] Le Pen *et al.* use on-train measurement of vertical track geometry through bogie acceleration readings to identify changes in track stiffness after track renewal. These track geometry measurements are corroborated by measurement of individual sleeper deflections using geophones and digital image correlation.[16] Significant variation in track stiffness is found in the transition zone between regular ballasted track and a level crossing, due mainly to the presence of a hanging sleeper.

Continuous drive-by track monitoring using in-service trains can provide information on track condition as a by-product of train operation at regular intervals. Recent improvements in the efficiency of wireless data transmission offer the potential of real time information feedback on track condition from in-service trains. This information can complement existing measuring techniques and be used to enable preliminary identification of track issues as they begin to occur. Weston *et al.*[1] predict that information gathered from in-service vehicles, in combination with other sources, will be

used to predict when an asset will require maintenance rather than scheduling maintenance based on the detection of track faults.

Cross-Entropy (CE) combinatorial optimisation is the method used in this paper to infer track stiffness profiles. The CE method is chosen as it is very effective at finding the global minimum for multi-variable problems where there are many local minima. The CE method is used to solve varied Civil Engineering problems. Harris *et al.*[17] use CE optimisation to infer road profiles using accelerometer readings characterising the vehicle response. O'Brien *et al.*[18] use CE optimisation to detect damage in road bridges by calculating an apparent bridge profile from Traffic Speed Deflectometer measurements.

Variation in stiffness along a track excites a dynamic response in a train which can potentially be used to determine that stiffness variation. A method is proposed in this paper for the detection of track stiffness variation through an analysis of in-service vehicle accelerations resulting from the vehicle-track dynamic interaction. The method is referred to throughout the paper as the Track Stiffness Measurement Algorithm (TSMA). A half-bogie 2D vehicle model is used to simulate vehicle track interaction. The resulting vehicle response is used as the simulated measurement and a half-bogie model uses this simulated measurement to back-calculate the stiffness profile. Measured track stiffness data is used as input into the algorithm to test its capabilities.

The authors are in the process of acquiring accelerometers to attach to an Irish Rail train so that in-service vehicle response can be obtained from a section of track in the form of vertical acceleration measurements. It is planned to use this data as input to the TSMA to infer the stiffness profile of the track. It is hypothesised that the application of the TSMA using many measured signals will, over time, increase the accuracy of the global track stiffness estimate.

2 MODEL DESCRIPTION

2.1 Vehicle Model

A half-bogie vehicle model, shown in Figure 1 is used in this study. The vehicle consists of three masses, m_c representing a quarter of the carriage body mass, m_b representing half the bogie frame mass and m_w representing the mass of the wheelset. The model has 3 degrees of freedom (DOF), corresponding to vertical translation at each mass. The carriage body and bogie frame are connected with an elastic spring, k_s and damper, c_s representing the secondary suspension of the vehicle. The bogie frame and wheelset are connected with an elastic spring, k_p and damper, c_p representing the primary suspension of the vehicle. An additional spring, k_H is used at the wheel rail contact. The stiffness of this 'contact spring', also known as a Hertzian spring, is defined as non-linear and varies according to the contact force between the wheel and the rail and the size of the elliptical contact patch.[19] However, some authors[20–22], choose to use a constant stiffness value for the Hertzian spring and a constant stiffness value of 1.4×10^9 N/m is used in this paper. This simplified representation of the vehicle aims to describe the dynamic behaviour of a railway vehicle and is taken from another study.[23] Vehicle properties for the locomotive configuration of a Thalys high speed train are listed in Table 1 and have been obtained from a recently published study using the same vehicle model.[24]
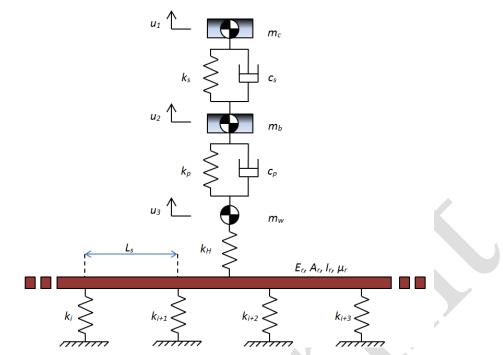
Figure 1 – Coupled 'Half-Bogie' vehicle model and beam-on-elastic-foundation track model

Table 1 – Properties of the vehicle

Property	Unit	Symbol	Value
Mass of carriage body	kg	m_c	13 400
Mass of bogie frame	kg	m_b	1 600
Mass of wheelset	kg	m_w	2 000
Damping of Primary Suspension	Ns/m	c_p	20 000
Damping of Secondary Suspension	Ns/m	c_s	5 000
Stiffness of Primary Suspension	N/m	k_p	$0.61{\times}10^6$
Stiffness of Secondary Suspension	N/m	k_s	$1.05{\times}10^6$
Hertzian Spring Stiffness	N/m	k_H	$1.4{\times}10^9$

The equations of motion of the vehicle can be defined by a set of second order differential equations:

$$\mathbf{M_v}\ddot{u}_v + \mathbf{C_v}\dot{u}_v + \mathbf{K_v}u_v = f_v \tag{1}$$

where $\mathbf{M_v}$, $\mathbf{C_v}$ and $\mathbf{K_v}$ are the mass, damping and stiffness matrices of the vehicle respectively and $\ddot{u}_v$, $\dot{u}_v$ and u_v are vectors of vehicle accelerations, velocities and displacements respectively. f_v is the time-varying dynamic interaction force vector.

2.2 **Track Model**

The TSMA uses a beam-on-elastic-foundation model featuring a single layer of discrete elastic springs so that a global track stiffness profile can be returned. This allows for variations in all track features (e.g. ballast thickness, subgrade strength) to influence the returned global stiffness profile.

The beam-on-elastic-foundation track model features an elastic beam (the rail) continuously supported on a series of springs with varying stiffness $\boldsymbol{k}$ as shown in Figure 1. Track supports are spaced at a regular interval, L_s, representing the spacing between the sleepers. A UIC60 rail is modelled as a finite element Euler-Bernoulli beam with one beam element per sleeper spacing. Each track element has 2 nodes with 2 degrees of freedom (DOF), vertical translation and rotation, at each node. Rail irregularities are likely to have a significant effect on the acceleration signal but are not considered in this investigation. The effect of rail irregularities will be investigated in a future study.

Values used in this study are taken from Zhai et al.[25] and are listed in Table 2. Note that properties marked with an asterisk (*) in the table are for single rail only and are doubled in order to include both rails in the planar model.

Table 2 – Properties of the rail (*Value for single rail only)

Property	Symbol	Value	Unit
Elastic modulus of rail	E_r	2.059×10^{11}	N/m^2
Rail cross-sectional area	A_r	7.69×10^{-3}	m^2
Rail second moment of area	I_r	*3.217×10^{-5}	m^4
Rail mass per unit length	μ_r	*60.64	kg/m
Sleeper Spacing	L_s	0.545	m

The equation of motion for the track model can be defined by a set of second order differential equations:

$$\mathbf{M_t}\ddot{u}_t + \mathbf{C_t}\dot{u}_t + \mathbf{K_t}u_t = \mathbf{N_t}f_{int} \tag{2}$$

where $\mathbf{M_t}$, $\mathbf{C_t}$ and $\mathbf{K_t}$ are the mass, damping and stiffness matrices of the track respectively and $\ddot{u}_t$, $\dot{u}_t$ and u_t are vectors of track accelerations, velocities and displacements respectively. f_{int} contains the total interaction forces between the vehicle and the track at their contact points. $\mathbf{N_t}$ is a location matrix used to distribute the vehicle load to the DOF's of the rail and is calculated using Hermitian shape functions. This method of distribution is well documented in the literature.[26,27]

2.3 Coupled Model

The vehicle and track subsystems are combined to form a coupled vehicle-track interaction model (Figure 1). The equations of motion for the coupled vehicle-track model are defined by a set of second order differential equations that are represented in matrix format as:

$$\mathbf{M_g}\ddot{u} + \mathbf{C_g}\dot{u} + \mathbf{K_g}u = F \tag{3}$$

where $\mathbf{M_g}$, $\mathbf{K_g}$ and $\mathbf{C_g}$ are the global mass, stiffness and damping matrices respectively and $\ddot{u}$, $\dot{u}$ and u are the vectors of system accelerations, velocities and displacements. F is the coupled system force vector. It is assumed that the vehicle always maintains contact with the rail – decoupling is not considered in this article. Due to the coupling between the vehicle and the track, the system stiffness matrix $\mathbf{K_g}$ is time-varying and is recalculated in every time step. A static analysis is carried out before a dynamic analysis is initiated. The equations of motion are solved using the Wilson-θ numerical integration scheme[28,29] with a time step of 1 ms corresponding to a sensor scanning frequency of 1000 Hz. A value of $\theta = 1.420815$ is used to ensure unconditional stability of the algorithm.[30] The model is implemented in Matlab.

3 METHODOLOGY

Local variation in track stiffness can generate a low-frequency change in vehicle riding response. It follows that the vehicle response can be used to infer the change in track stiffness. A railway TSMA is described in this section to test this concept. The algorithm uses as input a vehicle vertical acceleration signal generated using the models described in Section 2. Variation of track stiffness is introduced by varying the track stiffness vector $\mathbf{k}$ in the track model.

3.1 Basis for structure of the TSMA

As stated in Section 2.2, the TSMA uses a beam-on-elastic-foundation model to return a global track stiffness profile. This allows for variations in all track features (e.g. variation in ballast thickness, variation in subgrade strength) to influence the returned global stiffness profile. The optimisation algorithm uses a population based iterative procedure and a simple track model is used to optimise computational efficiency. To determine the length of the track model used in the algorithm, the bending stiffness of the rail must be considered. Zimmermann[31] shows that the deflection, u_r, of an infinitely long rail on an elastic foundation model under a single wheel load, P is given by:

$$u_r(x) = \frac{PL^3}{8EI}\mu(x) \tag{4}$$

where EI is the bending stiffness in the rail, x is the position along the track (wheel load is positioned at $x = 0$), and L is the so-called characteristic length given by:

$$L = \sqrt[4]{\frac{4EIL_s}{k_d}} \tag{5}$$

where k_d is a spring constant of a discrete support with a constant spacing, L_s. $\mu(x)$ is a shape function defining the shape of the deflection of the rail in the vicinity of the point load given by:

$$\mu(x) = e^{-x/L}\left[\cos\left(\frac{x}{L}\right) + \sin\left(\frac{x}{L}\right)\right] \qquad x \geq 0 \tag{6}$$

Due to the bending stiffness in the rail, the deflection of the track can be positive and negative (uplift of the rail). Deflections to the left of the point load ($x < 0$) are calculated from symmetry about the point load location ($x = 0$)[22]. Figure 2 uses a dashed line to show an approximation of the deflected shape of a rail under a wheel load, P. The high bending stiffness of the rail distributes the wheel load over a number of sleepers.
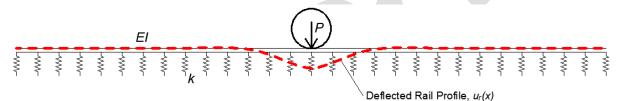

Figure 2 –Deformation due to point load for a beam-on-elastic-foundation model.

The track stiffness over this section has an influence on the track deflection and, by extension, the vehicle response. It is therefore necessary to include a number of sleepers at the beginning and end of the model to account for the boundary effects that the rail bending stiffness creates. Eqn. 5 shows that a reduction in the track stiffness increases the characteristic length and therefore the distribution of the load on the track. Depending on the magnitude of the point load, significant deflection in the rail is observed at up to $6L$ in both directions from the point load (for typical train loads)[22]. Table 3 provides a sample of characteristic lengths calculated from different track stiffnesses for a sleeper spacing L_s equal to 0.545m. As a result of this analysis, 15 sleepers are included before and after the vehicle start and end positions to provide the TSMA with an adequate detection range. This boundary length has also been used in another track stiffness study.[4]

Table 3 – Number of Sleepers required based on characteristic length for alternative discrete track stiffnesses values

k_d (kN/m)	EI (kNm²) (UIC60)	L (m)	$6L$ (m)	No. Sleepers
10 000 000	13 248	0.232	1.391	3
1 000 000	13 248	0.412	2.473	5
100 000	13 248	0.733	4.399	8
10 000	13 248	1.303	7.822	15

As discussed in Section 1, track stiffness k varies longitudinally along a section of track and is, in general, different at each sleeper location. Therefore, the track stiffness profile is represented by a track stiffness vector $\boldsymbol{k}$, and the components of the track stiffness vector vary along a section of track. The determination of $\boldsymbol{k}$ is a challenging multi-variable problem. Allowing for 15 sleepers at the start and end of the test section, the total number of components of $\boldsymbol{k}$ is the nearest integer value to, $30 + L_t/L_s$, where L_t is the length of the test section and L_s is the sleeper spacing.

To reduce the number of variables defining the stiffness vector, a track stiffness profile template is used. In this paper, the shape of a normal distribution function is used as the track stiffness profile

template. The choice of this function does not have any statistical relevance; it is selected because it can be used to represent a smoothly varying fall (or gain) in stiffness. The change in stiffness can be either gradual or rapid. It is represented here using three variables: location, width and scale, as illustrated in Figure 3. The way in which the track stiffness profile template is affected by the adjustment of the individual variables is shown in Figure 3 (a,c,e). The corresponding bogie acceleration signals produced by the VTI over these profiles are shown in Figure 3 (b,d,f) illustrating the effect of adjusting the variables. The cyclic variation in the acceleration signals represents the frequency of the track sleeper spacing.

Variable A, location, corresponds to the mean of the normal distribution function in statistics. Variable B, width, relates to the standard deviation of the normal distribution while a scaling factor, Variable C, is applied to vary the magnitude of the change in stiffness and define its sign (positive or negative change). By using the normal distribution function as a template to measure the variation of track stiffnesses the number of stiffness components to be determined is reduced from some tens to just three (Only one local variation in stiffness is found in each optimisation).
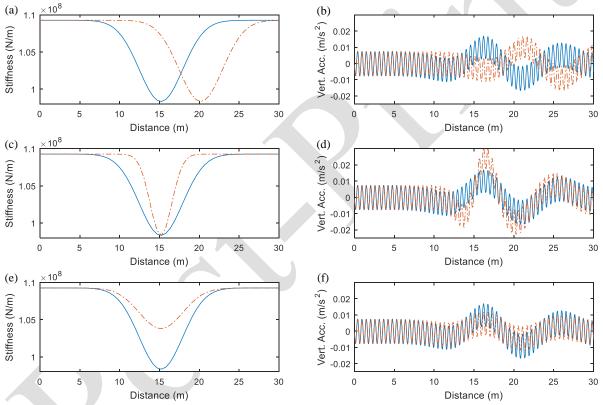

Figure 3 – Effect of track stiffness profile template variables on bogie DOF acceleration signal; a – Track stiffness profile: Vary avriable A: Location; b – Acceleration signal: Effect of varying location; c – Track stiffness profile: Vary variable B: Width; d – Acceleration signal: Effect of varying width; e – Track stiffness profile: Vary variable C: Scale; f – Acceleration signal: Effect of varying scale.

3.2 Cross Entropy Optimisation

The Cross-Entropy (CE) combinatorial optimisation technique is used in this paper to return a track stiffness profile from the dynamic measurements as a vehicle crosses a track. In this application, CE is used to find the stiffness vector which minimises the sum of squares of differences between the simulated measured and theoretical acceleration signals. Generally stated, the CE method is an iterative procedure which firstly generates a population of trial solutions (a population of stiffness vectors) according to a specified random mechanism and then updates the parameters of the random mechanism to produce an improved population of solutions in the next generation.[32] The goal is that, over several generations, the population converges to a global minimum. The method has been successfully applied to a various Civil Engineering problems.[17,33] An illustration of the CE concept is provided in Figure 4.
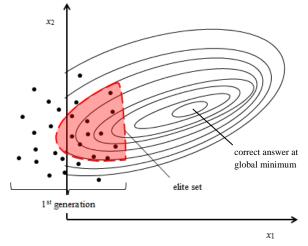
Figure 4 – Illustration of the Cross Entropy method – 1st generation

In this study the 'measured' acceleration signal is taken from the simulated measured response of a half-bogie vehicle traversing a track model. The measured acceleration signal is taken as the bogie vertical DOF. In their review of railway track geometry condition monitoring from in-service railway vehicles, Weston *et al.*[1] advise that sensors located on the sprung mass tend to provide the best compromise between sensor maintenance and quality of signal with respect to noise.

A population of the three variables defining the shape of the stiffness profile variation (location, width and scale) is generated in a Monte Carlo simulation. For each group of variables in the population, a vehicle track dynamic interaction is simulated, returning an acceleration signal for the bogie DOF. An objective function is then evaluated to determine the quality of the fit of each trail acceleration signal generated to the simulated measured acceleration signal. In this paper the objective function, O, (Eqn. 7) is simply taken as the sum of the squares of the differences between accelerations calculated for each trial stiffness profile, $\ddot{u}_{trial,t}$, and the simulated measured acceleration signal, $\ddot{u}_{meas,t}$:

$$O = \sum_{t=1}^{T} \left(\ddot{u}_{trial,t} - \ddot{u}_{meas,t} \right)^2 \tag{7}$$

where *t* is the scan number, and *T* is the total number of scans in the acceleration signal. The objective function values for each stiffness profile in the population are ranked and the elite set of variables defining the trial stiffness profiles identified. From trial and error, an elite set size of 10 is found to be effective. The population mean and standard deviation of the elite set are calculated and used to generate an improved population of stiffness distributions in the next generation. This process is repeated until convergence is achieved. Convergence is said to have been achieved when the mean values of the variables defining the stiffness profile location, width and scale do not change significantly between generations. Convergence criteria can be varied according to the accuracy desired. The population and elite set size can be varied and have an influence on the accuracy and execution time of the algorithm. The majority of the computational effort expended in executing the TSMA is spent simulating the VTI for each stiffness profile in the population. Therefore running the TSMA with a small population requires less time to execute, compared to a large population.

Once the optimisation has converged within a phase (see Section 3.3), a solution of variables defining the best fit stiffness profile is returned. To ensure that the TSMA has not prematurely converged to an incorrect solution the optimisation is restarted using the results of the variables from the previous optimisation within that phase as the mean values for the generation of new variables. The initial population standard deviations for each variable remain constant for each restart. The algorithm proceeds to the next phase only when matching solution sets for two subsequent optimisations are achieved.

Figure 5 graphically represents the calculation of the objective function. In Figure 5a-b the true stiffness profile used for this example and the corresponding 'measured' acceleration signal generated by the VTI model using the true profile are shown. In Figure 5(c,e), two trial solutions from the population of theoretical stiffness profile variables are shown with their corresponding theoretical acceleration signals shown in Figure 5(d,f). The Objective Function values are calculated and shown in the figure, with a smaller value indicating a stiffness profile closer to the true one.
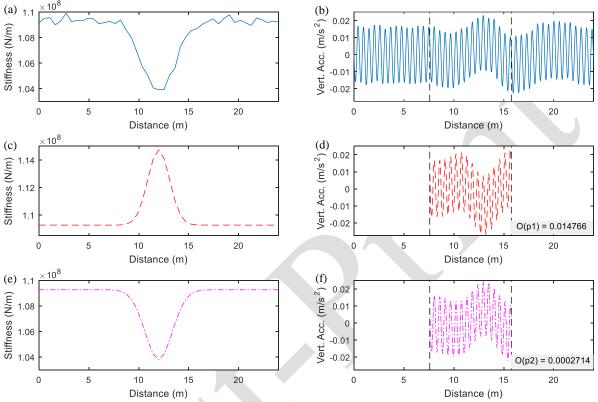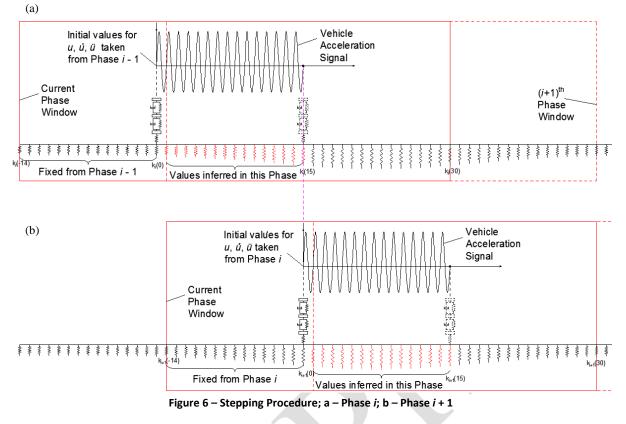

Figure 5 – Graphical representation of Objective Function calculation; a – true stiffness profile, b – measured vehicle response, c – 1st trial theoretical stiffness profile (p1), d – theoretical vehicle response to 1st trial and Objective Function value O(p1), e – 2nd trial theoretical stiffness profile (p2), f – theoretical vehicle response to 2nd trial and Objective Function value O(p2)

3.3 **Stepping through the track stiffness profile**

Railway track stiffness varies along a track and may contain multiple local features – local troughs or increases in stiffness. It is only possible to determine one such feature per optimisation using the proposed technique. Therefore it is required to step through the profile in phases so that multiple features can be determined along the length of the track. The track model used in the TSMA is limited to 45 sleepers in length so that stiffness values can be found for the central 15 sleepers and the bending effects of the rail can be accounted for at the edges by adding 15 sleepers at each end. The TSMA 'steps' through the profile in phases as shown in Figure 6 using the stiffness profile template, and outputs an estimate of the true track stiffness profile for each individual section. The estimate of the true track stiffness profile for a full length of track is constructed by combining the estimates from the smaller track sections.

Figure 6 – Stepping Procedure; a – Phase *i*; b – Phase *i* + 1

The components of the global track stiffness vector are returned at sleeper locations. Stiffness values for the central 15 sleepers inferred in Phase *i* are used as specified stiffness values for the first 15 sleepers in Phase *i* + 1. Initial values for model displacement, velocity and acceleration vectors calculated from the VTI for best-fit stiffness profile determined in Phase *i* are transferred to Phase *i* + 1 so that the vehicle is already in dynamic equilibrium at the start of each phase. The model vectors are transferred from an equivalent vehicle position in the previous phase. Referring to Figure 6, model vectors are taken from the first vehicle position after sleeper $k_i(15)$ in Phase *i* and transferred to an equivalent position after sleeper $k_{i+1}(0)$ in Phase *i* + 1. The stiffness values determined in each phase are assembled to determine the overall track stiffness profile over a finite length of railway track.

In Phase 1 an additional variable, *D*, is required to provide a baseline track stiffness value so that the first 15 values of the stiffness profile can be determined prior to initialisation of the second phase. This variable is no longer required in the second and subsequent phases as stiffness values for the first 15 sleepers are known from Phase 1. Parameters used in the Cross Entropy optimisation are listed in Table 4.
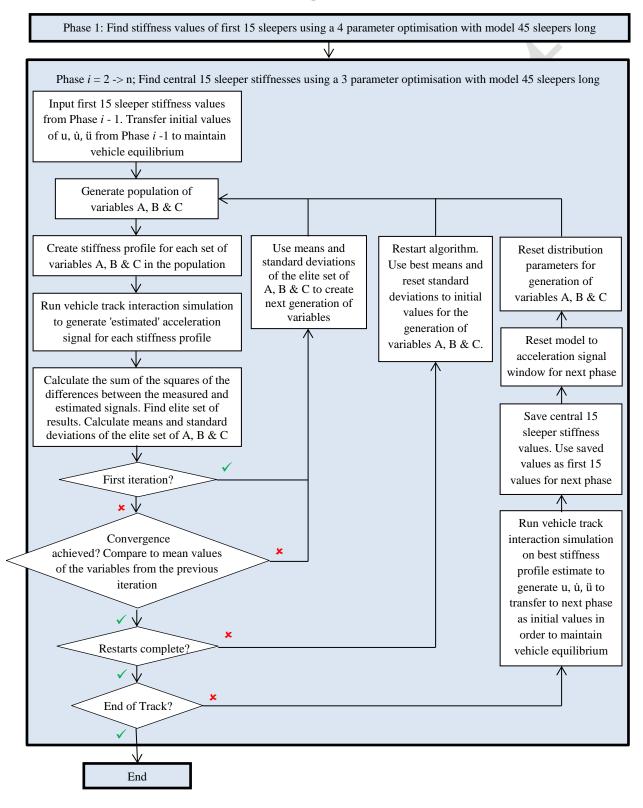
In each phase, the method attempts to find the best fit distribution of stiffness over the last 30 sleepers and, once convergence is reached, retains the central 15 sleepers as the inferred track stiffness values for the phase. As a result the method is limited to finding either one sudden change in track stiffness (such as a hanging sleeper) or a gradual change in track stiffness over a track distance of 15 sleepers (8.175 m). Therefore the method has the potential to cope with some track stiffness variations found in other studies[13,16] but testing using real field data is required to confirm this hypothesis. This will be the subject of a future paper. An increase in the resolution of the method can be achieved by reduction in the phase step size (i.e. reduction of the number of sleepers in the central section of the track model) but this comes at a computational cost.

Table 4 – Optimisation Parameters

Property	Value/ Population initial mean	Population initial standard deviation
Global track stiffness values inferred per phase (at sleeper locations)	15	-
Number of best fit solutions used to update variables	10	-

Variable A (Location)	0	25
Variable B (Width)	2.5	5
Variable C (Scale)	0	1×10^8

3.4 **TSMA Structure**

A flowchart describing the overall process for the TSMA is provided in Figure 7. A vehicle-track interaction (VTI) is simulated on a known stiffness profile to generate the measured acceleration signal, prior to initialisation of the TSMA. This 'measured' acceleration signal is then input into the TSMA which returns an inferred track stiffness profile.

Figure 7 – TSMA Flowchart

4   RESULTS AND DISCUSSION

The results of a number of numerical tests of the TSMA are presented in this section. The capabilities of the algorithm are first tested in Section 4.1 using a simulated measured vehicle acceleration signal generated using a VTI between the half-bogie vehicle model and a track model featuring an idealised variation in track stiffness. In Section 4.2, measured track stiffness data is used as the stiffness vector k in the track model and a VTI is simulated to generate a more realistic measured vehicle acceleration signal. The effect of population size on TSMA accuracy is presented in Section 4.3 while resilience to measurement noise, and uncertainty in vehicle properties are investigated in Section 4.4 and Section 4.5 respectively.

4.1   **Idealised Variations in Track Stiffness Profile**

This section presents the result of a TSMA simulation using a half-bogie vehicle acceleration signal generated from crossing a beam-on-elastic-foundation track model with an idealised variation in the true stiffness profile. A stiffness profile featuring three variations in track stiffness, each with a normal distribution function shape, are spread along a 140 m length of track. As shown in Figure 8, the TSMA successfully estimates the true track stiffness profile. The vehicle speed is 120 km/h. Gaussian signal noise (3%, SNR = 30.5 dB) is added to the 'measured' vehicle acceleration signal before initiating the TSMA. A population of 750 estimates is used for the optimisation of each phase. The computation time required for the TSMA to infer the track stiffness profile was 11 hours with a 2.4 GHz processor, 16.0 GB RAM running on Matlab.
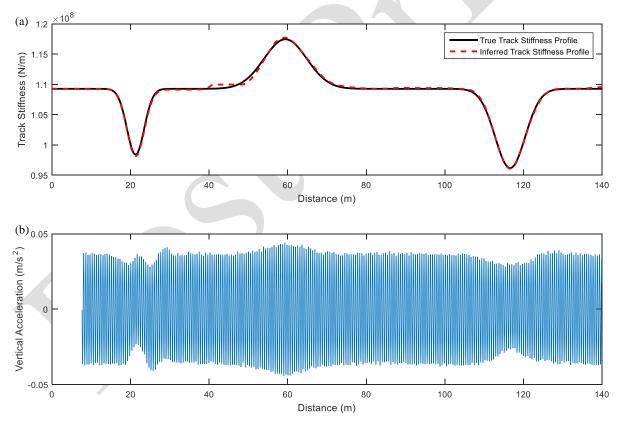

Figure 8 – a – True and Inferred Track Stiffness Profile – Idealised change in True Track Stiffness Profile; b – Measured bogie DOF vertical acceleration

4.2 Measured Track Stiffness Data

This section presents the results of TSMA simulations using track stiffness data for a section of track between Gothenburg and Alingsås, Sweden, gathered using the Rolling Stiffness Measurement Vehicle (RSMV). The data shown was measured by the RSMV[34] with a dynamic excitation of 6 Hz at a speed of 20 km/h. Before initiating the TSMA a VTI is carried out using the half-bogie vehicle travelling at a speed of 120 km/h across a beam-on-elastic-foundation track model 1.5 km in length. Discretised track stiffness values interpolated from the Swedish data are used as the stiffness vector in the track model. In a realistic situation the measured stiffness value is an estimation of the true stiffness and is a function of the various parameters of the method of measurement and measurement error.

Gaussian signal noise (3%, SNR = 30.5 dB) is added to the 'measured' vehicle acceleration signal before initiating the TSMA. A population of 400 estimates is used for the optimisation of each phase. The computation time required for the TSMA to infer the track stiffness profile was approximately 40 hours. Figure 9 shows the results of the simulation. An excellent fit between the true and the inferred track stiffness profile is achieved. The root of the sum of squared differences between the true track stiffness $\boldsymbol{k}_t$ and the inferred track stiffness $\boldsymbol{k}_{inf}$ profile, divided by track length, is used to quantify the margin of error between the true and inferred profiles (Eqn. 8).

$$E_{RSS} = \frac{\sqrt{\sum_{x=1}^{S}(\boldsymbol{k}_t - \boldsymbol{k}_{inf})^2}}{SL_s} \tag{8}$$

where S is the number of sleepers inferred and L_s is the sleeper spacing. An error of 52 176 N/m/m is achieved for the inferred track stiffness profile shown in Figure 9.
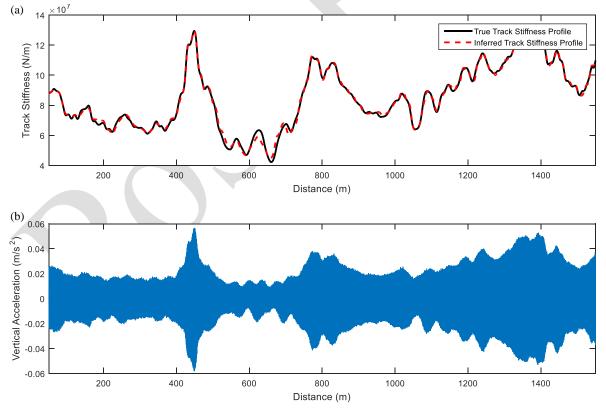

Figure 9 – a – True and Inferred Track Stiffness Profile – Swedish Track Stiffness Data; b – Measured bogie DOF vertical acceleration

4.3 Influence of Population Size

As stated in Section 3.2, the size of the population of estimates has an influence on the accuracy and speed of execution of the TSMA. This hypothesis is tested in this section. Track stiffness data for a different section of track between Gothenburg and Alingsås, Sweden, is used as the stiffness data for the generation of the measured signal. Before initiating the TSMA, a VTI is carried out using the half-bogie vehicle travelling at a speed of 120km/h across a beam-on-elastic-foundation track model 350 m in length. Gaussian signal noise (3%, SNR = 30.5 dB) is added to the 'measured' vehicle acceleration signal before initiating the TSMA for a range of population sizes.

Figure 10a shows the results of the analysis for a range of population sizes. There is clear relationship between TSMA accuracy and population size, with increased accuracy for larger population sizes. However, larger populations also increase the run times as illustrated in Figure 10b. It can be observed that a population of 100 or more provides an acceptable level of error while keeping execution times to a minimum.
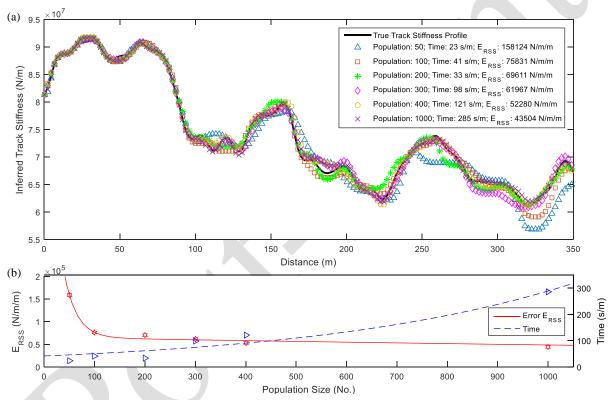

Figure 10 – Influence of TSMA population size; a – Inferred track stiffness profiles; b – Root of the Sum of Squared differences Error (E$_{RSS}$) and run times vs. population size

4.4 **Influence of Measured Signal Noise**

Any real system used to measure vehicle response will be subject to measurement noise. Therefore the TMSA must have some tolerance to measurement noise if it is to be implemented using real measured vehicle data at a future stage. For this analysis increasing levels of measurement noise are added to the simulated measured acceleration signal before initiating the TSMA. Measured track stiffness data for a different section of track between Gothenburg and Alingsås, Sweden, is used as the stiffness data for the generation of the measured signal. As before, a VTI is carried out using the half-bogie vehicle travelling at a speed of 120 km/h across a beam-on-elastic-foundation track model 350 m in length. Increasing Gaussian signal noise levels of 0%, 1%, 3%, 5% and 10% (SNR = ∞, 40 dB, 30.5 dB, 26 dB and 20 dB) are added to the 'measured' vehicle acceleration signal before initiating the TSMA.

Figure 11 presents inferred stiffness profiles and accuracy values for a range of added signal noise levels. A population of 100 was used for all simulations. It can be seen that an increase in the level of measurement noise results in a small but tolerable reduction in the accuracy of the inferred stiffness profile, even for a measurement noise level of 10%. There is also an increase in the time of execution for higher levels of added signal noise.
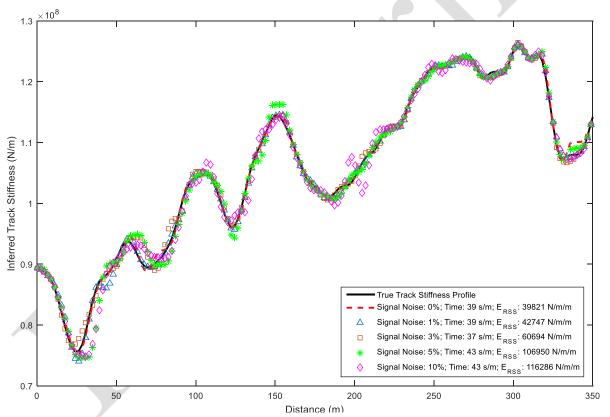

Figure 11 – Influence of added signal noise on inferred track stiffness profiles

4.5 **Influence of Vehicle Property Uncertainty**

When using the response of a vehicle crossing a track to infer information on track properties it is necessary to have an accurate knowledge of the vehicle properties. The mass of various vehicle components can be accurately measured. However the mass of the carriage and its distribution to the front and rear bogies will vary according to fuel loading and passenger numbers and seating location. Also, it is not always possible to obtain accurate values for suspension properties, especially when using an idealised vehicle model as is done in the TSMA. Therefore the TMSA must have some tolerance to variation in the mass and suspension properties of the vehicle model. Absi and Mahadevan present various methods for determining model parameters and stress the importance of accurate determination of model parameters to minimise differences between model outputs and experimental data.[35] In this section of the paper the effect of two different levels of vehicle parameter uncertainty are considered. Parameter uncertainty is modelled as random noise applied to the actual vehicle parameters.

Measured track stiffness data for a different section of track between Gothenburg and Alingsås, Sweden, is used as the stiffness data for the generation of the measured signal. As before, a VTI is carried out using the half-bogie vehicle travelling at a speed of 120 km/h across a beam-on-elastic-foundation track model 350 m in length. Gaussian signal noise (3%, SNR = 30.5 dB) is added to the 'measured' vehicle acceleration signal. Gaussian noise levels of 3% (SNR = 30.5 dB) are also added to vehicle mass, stiffness and damping properties before initiating the TSMA. The process is repeated for a uncertainty level of 6% (SNR = 24.4 dB) on the same vehicle properties.

The TSMA is executed 5 times for each level of noise and the results of the analysis are presented in Figure 12. It can be seen that an increase in the level of uncertainty on vehicle properties widens the ±1 standard deviation band within which 68% of estimates will occur. The authors acknowledge that more simulations of the TSMA are necessary to improve the accuracy of this distribution but long model execution times prevented a more extensive statistical analysis. Nevertheless, even based on 5 sets of results, it can be seen from the comparison of the 3% and 6% uncertainty bands in Figure 12c that a 3% error in vehicle properties is tolerable but a 6% error may present some issues with the accuracy of the algorithm.
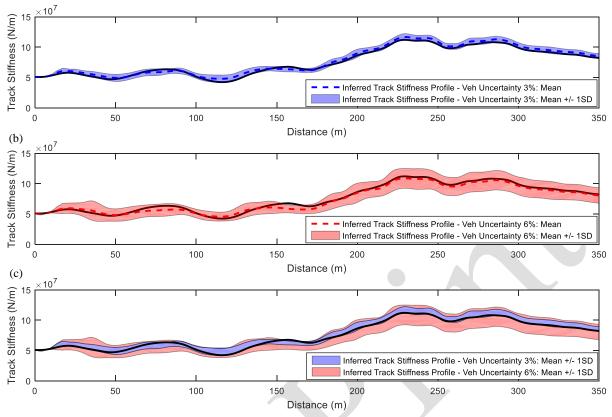
(a)

Figure 12 – Influence of vehicle property uncertainty on inferred track stiffness; True stiffness profile shown as solid black line; a – Inferred stiffness profile with 3% vehicle property uncertainty; b – Inferred stiffness profile with 6% vehicle property uncertainty; c – Comparison of 3% and 6% vehicle property uncertainty results

5   CONCLUSIONS

Longitudinal variation in railway track stiffness causes a change in vehicle riding response. It follows that a measured acceleration signal characterising this response can potentially be used to determine the stiffness variation. In this paper, a novel method for measuring a track stiffness profile using measurements of vehicle acceleration has been described. The Track Stiffness Measurement Algorithm (TSMA) employs a Cross-Entropy optimisation technique to infer the global track stiffness profile by optimising a stiffness variation shape, used as a template to fit to the true track stiffness profile over short sections of track. The TSMA steps along the railway track in phases and combines the individual inferred profiles from each phase into an overall inferred stiffness profile for the track. The stiffness variation template used in this study is the normal distribution function.

From the results shown in this paper, it can be concluded that the TSMA has the potential to be used to estimate local variations in railway track stiffness using vehicle acceleration data. Actual measured stiffness data, combined with numerical models to calculate simulated measured acceleration signals, are used to test the algorithm for real-world variations in track stiffness. The TSMA performs well for various levels of added signal noise, and uncertainty in vehicle properties.

In its current form the TSMA does not have the computational efficiency required to provide continuous feedback from an in-service system. Significant improvements in efficiency and computing power, perhaps achievable through parallel computing, are required before in-service operation becomes a reality. In the meantime, vehicle accelerations recorded at some regular cycle, i.e. monthly or quarterly, could be post-processed to return track stiffness information. Accurate estimation of variations in railway track stiffness using sensors mounted on in-service vehicles has the potential to provide a valuable tool to inform maintenance planning and address other infrastructural problems such as railway track settlement.

6   ACKNOWLEDGEMENT

7   REFERENCES

1.   Weston P, Roberts C, Yeo G, et al. Perspectives on railway track geometry condition monitoring from in-service railway vehicles. *Veh Syst Dyn Int J Veh Mech Mobil* 2015; 53: 1063–1091.

2.   Oscarsson J, Dahlberg T. Dynamic train/track/ballast interaction - computer models and full-scale experiments. *Veh Syst Dyn Int J Veh Mech Mobil* 1998; 29: 73–84.

3.   Dahlberg T. Track issues. In: Iwnicki SD (ed) *Handbook of railway vehicle dynamics*. Taylor & Francis, 2006, pp. 143–197.

4.   Dahlberg T. Railway track stiffness variations–consequences and countermeasures. *Int J Civ Eng* 2010; 8: 1–12.

5.   Selig ET, Waters JM. *Track Geotechnology and Substructure Management*. Thomas Telford, 1994.

6.   Selig ET, Li D. Track modulus: its meaning and factors influencing it. *Transp Res Rec 1470* 1994; 47–54.

7.   Hosseingholian M, Foumentin M, Robinet A. Dynamic track modulus from measurement of track acceleration by portancemetre. In: *9th World Congress on Railway Research*. France, 2011.

8.   Frýba L. *Vibration of solids and structures under moving loads*. 3rd ed. Prague: Thomas Telford, 1999.

9.   Frohling RD. *Deterioration of railway track due to dynamic vehicle loading and spatially varying track stiffness*. Ph.D. Thesis, University of Pretoria, South Africa, 1997.

10.   Hosseingholian M, Froumentin M, Levacher D. Continuous method to measure track stiffness a new tool for inspection of rail infrastructure. *World Applied Sciences Journal* 2009; 6: 579–589.

11.   IS EN 13848: Railway Applications - Track - Track Geometry Quality - CEN European Committee for Standardisation.

12.   Kolbe T, Kratochwille R. ICE-S - Vehicle reaction measurement and track geometry measurement on the same measuring train. Results of the comparison of the two different track inspection methods. In: *IMechE Stephenson Conference for Railways, London. Paper: C1408/068*. 2015.

13.   Murray CA, Take WA, Hoult NA. Measurement of vertical and longitudinal rail displacements using digital image correlation. 2015; 155: 141–155.

14.   Berggren EG. *Railway track stiffness – dynamic measurements and evaluation for efficient maintenance*. Ph.D. Thesis, Royal Institute of Technology, Sweden, 2009.

15.   Berggren EG, Nissen A, Paulsson BS. Track deflection and stiffness measurements from a track recording car. *J Rail Rapid Transit* 2014; 228: 570–580.

16.   Le Pen L, Watson G, Powrie W, et al. The behaviour of railway level crossings: Insights through field monitoring. *Transp Geotech*; 1: 201–213, http://linkinghub.elsevier.com/retrieve/pii/S2214391214000130 (2014).

17. Harris NK, González A, OBrien EJ, et al. Characterisation of pavement profile heights using accelerometer readings and a combinatorial optimisation technique. *J Sound Vib* 2010; 329: 497–508.

18. OBrien EJ, Keenahan J. Drive-by damage detection in bridges using the apparent profile. *Struct Control Heal Monit* 2014; 22: 813–825.

19. Iwnicki SD. *Handbook of railway vehicle dynamics*. Taylor & Francis, 2006.

20. Bowe C. *Dynamic interaction of trains and railway bridges using wheel rail contact method*. Ph.D. Thesis, National University of Ireland, Ireland, 2009.

21. Connolly D, Giannopoulos A, Forde MC. Numerical modelling of ground borne vibrations from high speed rail lines on embankments. *Soil Dyn Earthq Eng* 2013; 46: 13–19.

22. Esveld C. *Modern railway track*. 2nd ed. Delft: MRT-Productions, 2001.

23. Frýba L. *Dynamics of railway bridges*. London: Thomas Telford, 1996.

24. Kouroussis G, Verlinden O. Prediction of railway ground vibrations: accuracy of a coupled lumped mass model for representing the track/soil interaction. *Soil Dyn Earthq Eng* 2015; 69: 220–226.

25. Zhai WM, Wang KY, Lin JH. Modelling and experiment of railway ballast vibrations. *J Sound Vib* 2004; 270: 673–683.

26. Fish J, Belytschko T. *A First Course in Finite Elements*. London: John Wiley & Sons Ltd, 2007.

27. Liu GR, Quek SS. *The finite element method: a practical course*. Oxford: Butterworth-Heinemann, 2003.

28. Bathe KJ, Wilson EL. *Numerical methods in finite element analysis*. Englewood Cliffs, UK: Prentice Hall, 1976.

29. Tedesco JW, McDougal WG, Ross CA. *Structural dynamics, theory and applications*. California, USA: Addison Wesley Longman, 1999.

30. Weaver W, Johnston PR. *Structural dynamics by finite elements*. Indiana, USA: Prentice Hall, 1987.

31. Zimmermann H. *Die berechnung des eisenbahnoberbaues (The analysis of railway tracks, (in German)*. Verlag, W. Ernst & Sohn, Berlin, 1887.

32. de Boer PT, Kroese D, Mannor S, et al. A tutorial on the cross-entropy method. *Ann Oper Res* 2005; 134: 19–67.

33. Wilson SP, Harris NK, OBrien EJ. The use of Bayesian statistics to predict patterns of spatial repeatability. *J Transp Res Part C - Emerg Technol* 2006; 14: 303–315.

34. Berggren EG, Jahlénius Å, Bengtsson B-E, et al. Simulation, development and field testing of a track stiffness measurement vehicle. In: *Proceedings of 8th International Heavy Haul Conference*. Rio de Janeiro, 2005, pp. 763–772.

35. Absi GN, Mahadevan S. Multi-fidelity approach to dynamics model calibration. *Mech Syst Signal Process* 2016; 189–206.